

1 **CONDENSATION**

2 **TWEETABLE STATEMENT**

3 How to make a low-cost, high fidelity model to train for fetoscopic spina bifida repair. Fast,
4 clean, and portable setup allows surgical training anytime, anywhere.

5 **SHORT TITLE**

6 Low-Cost High-Fidelity Model for Spina Bifida Repair

7 **AJOG AT A GLANCE**

8 **A. Why was this study conducted?**

- 9 • To reduce the need for training on animals and allowing surgeons to attain
10 competency, we developed a high-fidelity synthetic model for training the
11 neurosurgical steps of fetoscopic spina bifida repair.

12 **B. What are the key findings?**

- 13 • A synthetic training model, complete with detailed instructions for replication is
14 now available.
- 15 • Skilled endoscopic fetal surgeons utilized the model for simulations and their
16 measured competency was maintained.

17 **C. What does this study add to what is already known?**

- 18 • Animal-based and low-fidelity training models for fetoscopic spina bifida repair
19 already exist.
- 20 • We developed a synthetic, reproducible, and low-cost high fidelity model.

21

22 **ABSTRACT**

23 BACKGROUND: Fetoscopic Spina Bifida repair (fSB-repair) is increasingly being practiced, but limited
24 skill acquisition poses a barrier to widespread adoption. Extensive training in relevant models,
25 including both *ex-* and *in-vivo* models may help. To address this, a synthetic training model that is
26 affordable, realistic and allows skill analysis would be useful.

27 OBJECTIVE: To create a high-fidelity model for training the essential neurosurgical steps of fetoscopic
28 spina bifida repair using synthetic materials. Additionally, we aimed to obtain a cheap and easily
29 reproducible model.

30 STUDY DESIGN: We developed a three-layered silicon-based model resembling the anatomical
31 layers of a typical myelomeningocele lesion. It allows for filling the cyst with fluid and conducting a
32 water tightness test post-repair. A compliant silicon ball mimics the uterine cavity, and is fixed to a
33 solid 3D printed base. The fetal back with the lesion (single-use) is placed inside the uterine ball,
34 which is reusable and repairable to allow practicing port insertion and fixation multiple times.
35 Following cannula insertion, the uterus is insufflated, and clinical fetoscopic, robotic or prototype
36 instruments can be used. Three skilled endoscopic surgeons each did six simulated fetoscopic repairs
37 following the surgical steps of an open repair. The primary outcome was surgical success, based on
38 water tightness of the repair, operation time <180 minutes and an Objective-Structured-Assessment-
39 of-Technical-Skills (OSATS)-score of $\geq 18/25$. Skill retention was measured using a competence
40 commulative sum (C-CUSUM) analysis on composite binary outcome for surgical success. Secondary
41 outcomes were cost and fabrication time of the model.

42 RESULTS: We made a model for simulating spina bifida repair neurosurgical steps with anatomical
43 details, port insertion, placode release and descent, undermining of skin and muscular layer, and
44 endoscopic suturing. The model is made with reusable 3D-printed molds with easily accessible
45 materials. The one-time startup cost was 211€, and each single-use simulated MMC-lesion costs 9.5€
46 in materials and 50 min working hours. Two skilled endoscopic surgeons performed six simulated

47 three-port fetoscopic repairs, while a third used a Da-Vinci surgical robot. Operation times decreased
48 over 30% from the first to last trial. Six experiments per surgeon did not show an obvious OSATS-
49 score improvement. C-CUSUM analysis confirmed competency for each surgeon.

50 CONCLUSION: This high-fidelity low-cost spina bifida model allows simulated dissection and closure
51 of a myelomeningocele lesion.

52

53 **INTRODUCTION**

54 Spina bifida aperta (SBA) is caused by incomplete neural tube closure during embryonic
55 development, leading to bladder and bowel dysfunction, motor and sensory impairment, skeletal
56 abnormalities, hindbrain herniation, ventricle enlargement, and cognitive impairments. Prenatal repair
57 has been explored to address SBA's progressive nature¹. There is level-1 evidence that, in selected
58 fetuses, prenatal repair reduces the need for ventriculoperitoneal shunt placement, improves
59 independent walking, volatile voiding, motoric function and independent functioning²⁻⁵. These data
60 were obtained in fetuses operated through a hysterotomy, which increases the risk of premature birth,
61 uterine dehiscence, and uterine rupture in the index or subsequent pregnancies⁶. To mitigate these
62 risks, less invasive techniques, e.g. mini-hysterotomy or minimally invasive approach have been
63 investigated⁷⁻⁹. While these alternative techniques are gaining acceptance¹⁰, there are still debates
64 regarding percutaneous or uterine exteriorization for fetoscopic repair¹¹⁻¹³. It is also noted that the
65 learning curve of fetoscopic repair seems to be twice as long¹⁴.

66 Transitioning to an endoscopic approach requires a training program, that in turn necessitates
67 a surgical training model. Typically, (endoscopic) surgical training first starts on computer simulators
68 or synthetic models (benchtop/box trainers) due to their low cost as compared to animals or human
69 cadavers, which also have ethical constraints and logistical challenges¹⁵. Creating realistic synthetic
70 models would simplify training logistics, reduce or even obviate the need for animal training, and
71 ensure competency before clinical practice. For fetoscopic spina bifida repair, several in-vivo high-
72 fidelity models including rabbits¹⁶, sheep¹⁷ and rhesus monkeys¹⁸ have been proposed. Three synthetic
73 trainers have been reported, of which two are referred to as low-fidelity^{19,20} and one as high fidelity
74 ²¹, although limited data on their use were reported. Herein, we aimed to develop a low-cost, high-
75 fidelity synthetic model capable of simulating all neurosurgical steps of a fetoscopic repair of a cystic
76 "myelomeningocele" lesion, i.e. placode release, skin excision, undermining the skin and muscle, and
77 closing the myofascial and skin layers. Additionally, we used the model to obtain baseline data from
78 experienced endoscopic surgeons performing simulated repairs.

79 **MATERIALS AND METHODS**

80 *Model description*

81 The model consists of 2 parts, (1) a single-use silicon replica of the fetal back with a cystic lesion in
82 the center and (2) a uterine cavity represented by a silicon ball tightly clamped to a 3D printed
83 reusable plastic base. The replica mimics clinical conditions present between 24 and 26 weeks
84 dimensionally²², with the lumbar region being the primary focus in 95% of cases and around half of
85 the lesions being cystic²³. The lesion measures 30x50 mm and has three layers of soft silicone (Figure
86 1(a)). The silicon used for the layers is EcoFlex 00-30 (Smooth-On, Macungie, PA) and the molds were
87 3D printed using fused deposition modeling (FDM) printers (Prusa I3 MK3S) and polylactic acid (PLA)
88 filament. The 3D printing was outsourced to a local fabrication lab (Fablab). The top layer (layer-3)
89 represents the skin with a cystic bulge and a placode (yellow pigmented region) measuring 20x10
90 mm²⁴. The cystic bulge is reinforced with a gauze mesh to prevent tearing when suturing. The middle
91 layer (pigmented red) represents the fascia with a small midline spinal defect just below the placode.
92 Cotton threads (yellow) are connected to the placode and inserted through the midline defect to exit
93 between the simulated fascia and the base silicone layer through two holes. This allows one to pull
94 on the threads once the placode has been freed, mimicking its descent into the spinal canal. These
95 threads also represent the nerves originating from the placode, so surgeons must avoid touching or
96 cutting these as well as the placode. The structures to the sides of the midline defect represent the
97 muscle flaps that are typically closed over the placode after undermining. The bottom layer forms a
98 water-tight cystic cavity. Layers are joined together using EcoFlex Gel (Smooth-On, Macungie, PA)
99 pigmented (Silc-pig™) with the color of blood, allowing separation similar to anatomical layers
100 (Supplementary video 1). A small tube between the base and middle layer serves as an inlet to fill the
101 cyst with water and assess water tightness post-repair. The replica of the fetal back and the silicone
102 ball are mounted on a solid 3D-printed base (Figure 1, Video 1).

103 The 3D printed plastic base is clamped to a surgical bed or table. A curved two centimeter high soft
104 silicon pad mimicking the lower back curvature, is placed over the base and under the cystic lesion. A
105 threaded plastic ring clamps the silicon cyst plate to the base, and the silicon ball is placed tightly
106 over the ring. This creates an air-tight seal for CO₂ insufflation. This air-tight simulated uterine cavity
107 can also be filled with water to simulate amniotic fluid and allow for ultrasound imaging.

108 Table 2 presents one-time costs of molds, parts, engineering hours and production time associated
109 with creating the model. Video 2 provides detailed instructions regarding the manufacturing of the
110 synthetic model, while video 1 shows the installation instructions and surgical steps during
111 endoscopic repair.

112 *Simulated surgical procedure*

113 The model is positioned on the operating table, and three ports are placed away from the placenta.
114 Although possible, ultrasound guidance for port placement is not included in the exercise as our
115 focus is on dry-lab and desktop training of neurosurgical steps. Surgeon may choose the distance
116 between ports and their location, based on their preferred approach developed during training.
117 During the procedure, an assistant holds the fetoscope and camera, while the surgeon handles the
118 instruments. With the Da Vinci robot (Intuitive, Sunnyvale, CA), no camera assistant is required.

119 Belfort et al. divided the surgical procedure in ten consecutive steps, of which only port insertion and
120 insufflation (step 2-3) and the neurosurgical steps (4 to 10)²⁵ are simulated herein (detailed in Table 1
121 and depicted in Figure 2). The repair is divided into five tasks: placode untethering and removal of
122 excessive skin, skin undermining, fascia mobilization, fascia closure and skin closure. The goal is to
123 achieve a water-tight closure over the released placode²⁶. Surgeon may choose preferred sequence
124 of surgical steps. The simulation may also include insertion of a dural patch prior to fascia closure, or
125 even to close the skin defect. Unfortunately we have not yet made a cheap replica of the patches
126 used to substitute for the expensive clinically used materials. Operation time of each step is noted,

127 and a leak test is performed by attaching an open syringe filled with water to the infusion tube and
128 raising to 35cm above the placode level to simulate the cerebrospinal fluid pressure²⁷.

129 *Surgeon, performance and fidelity scoring.*

130 We used this set up with three experienced endoscopic surgeons, routinely performing pediatric or
131 gynecologic surgery. All simulations were recorded and reviewed by an endoscopic surgeon (FDB,
132 blinded to the surgeon and sequence of trials) for time use and OSATS scoring²⁸. The OSATS scoring
133 assessed criteria such as: tissue respect (minimal damage to the placode and nerves), time and
134 motion, instrument handling and knowledge, and overall operation flow (Figure 3)^{12,26}. As model's
135 construct validity assessment, a composite binary outcome for surgical success, i.e. watertight
136 repair⁶, an repair time ≤ 180 minutes in accordance with the FDA Drug Safety Communication about
137 potential risks of general anesthesia in pregnant women²⁹ and an OSATS score $\geq 18/25$ ($>70\%$)^{12,26} was
138 calculated and used for the C-CUSUM analysis¹⁶.

139 Surgeons completed a questionnaire using a 5-item Likert-scale to assess model's realism (face
140 validity), utility (content validity), acceptability, and educational effect. Fidelity scale (Low-medium-
141 high) of a surgical simulator is not very well defined, and may depend on its likeness towards the
142 functional requirements of the clinical task rather than its educational value³⁰⁻³². Experience of the
143 trainee (expert vs. novice) may also affect the perceived fidelity of a model³³. Tun et. al argue that
144 high-fidelity does not require a faithful replication of the reality but rather an accurate
145 representation of real-world cues and stimuli³⁴. Based on requiring replication of the clinical scenario
146 (cystic defect and its repair) itself, we define our model as high-fidelity if the face and content validity
147 scores are rated $\geq 4/5$, medium-fidelity if $= 3/5$ and low-fidelity of $\leq 2/5$ on average.

148 **RESULTS**

149 We created a low-cost synthetic surgical training model with detailed reproduction instructions
150 (supplementary video 2). Initial material cost for reusable parts and molds is 211€ (table 2). The
151 single-use replica of the cystic spina bifida lesion and fetal back costs 9.5€ and takes 50 min to make.

152 The uterus can be reused by repairing cannula insertion sites (supplementary video 2) in 5 min and
153 negligible costs. The model has a quick 5 min setup time. It's a clean and portable desktop trainer
154 made of synthetic materials. The base can be mounted on any flat table or adjustable surgical beds,
155 allowing versatile positioning. It enables port insertion, simulates neurosurgical steps, placode
156 release and descent, undermining of skin and muscle layer, and endoscopic suturing. The model
157 displays anatomical details in color with realistic compliance properties (supplementary video 1).

158 After their six simulations, all surgeons rated the model's realism (face validity) positively in all
159 categories (uterine ball and lesion position, surgical tools, surgeon and assistant positioning), with
160 scores $\geq 4/5$. One surgeon rated fetoscopic vision realism as $=3/5$. Content validity scores for all
161 categories (realism and educational value of each surgical step, self-assessment) were also $\geq 4/5$. The
162 difficulty and stress of a clinical case received scores $\leq 3/5$ from all surgeons. Based on this user
163 feedback, we can confidently assert that the model demonstrates high fidelity in terms of both face
164 and content validity.

165 Figure 3 shows results from six training sessions by three skilled endoscopic surgeons. Despite the
166 low number of simulations, there was a significant reduction in operation time with increasing
167 experience, both in laparoscopy and robotics. On average, task completion time decreased by over
168 30%, with one surgeon achieving a 50% reduction. This improvement was not specific to certain
169 steps but overall. Interestingly, robotic experiments used significantly less CO₂ volume ($p < 0.001$). All
170 three surgeons remained proficient based on C-CUSUM analysis ($hC < 3$). However, with eight failed
171 exercises out of eighteen (Video 1), further practice on the model is needed. OSATS scores indicated
172 "tissue respect" as an important aspect, with scores below 18 coinciding with low "tissue respect"
173 scores ($n=7$). Robotic procedures excelled in "instrument handling" but scored low in "tissue
174 respect", seen through suture breakage in initial trials (Video 1).

175

176

177 **COMMENT**

178 *Principal findings*

179 For fetoscopic myelomeningocele repair, we developed a low-cost synthetic training model,
180 capable of simulating crucial surgical steps such as placode dissection, removal of excess
181 skin, undermining of skin and muscle flap, layer closure, and objective water tightness
182 testing. Experienced endoscopic surgeons ranked the model as “high fidelity”³⁴. Although
183 quite experienced with operative laparoscopy, the operation time of these surgeons
184 progressively diminished. However, neurosurgical “failures” still occurred. Interestingly, the
185 CO₂ volume used was significantly less for multi-arm robotic exercises, as well as instrument
186 handling scored higher within the OSATS score. Conversely the surgeon broke a few sutures,
187 which may be attributed to lack of haptic feedback and to which the surgeon eventually
188 adapts.

189 *Results in context of what is known*

190 Animal models are often used for training in spina bifida due to their high fidelity, but they
191 have limitations. For instance, the lamb spina bifida model¹⁷ lacks tissue required for primary
192 repair and can be expensive and logistically difficult to work with. Low-fidelity models, such
193 as the one described by Belfort³⁵, lacks the multiple layers required to simulate the clinical
194 procedure and is not suitable for dry-lab experiments. The Miller model¹⁹ can be used with a
195 silicon skin but only allows closure of the skin layer. The Surgical Touch³⁶ model also lacks the
196 multi-layered defect and is relatively more expensive. To our knowledge no evaluation of
197 these models is available. Spoor *et al.*²¹ proposed a high-fidelity synthetic model, with
198 features that allow for a layered repair and a model of the uterus. The report however lacks
199 details on reproduction, neither data on its use by surgeons. In this study, we present a

200 synthetic multi-layer model of the region of interest in a fetus with spina bifida, which is easy
201 to use and produce as well as low-cost. Experienced surgeons can use it to improve
202 confidence, shorten operation times, achieve watertight closure, and facilitate skill
203 development for novices or new team members. Our aim is to provide a realistic alternative
204 to animal models and promote ethical and sustainable surgical skill development.

205 *Clinical implications*

206 For complex and delicate procedures such as fetoscopic spina bifida repair, surgeons should
207 optimally prepare, logically first in a simulated environment. Neurosurgeons are quite
208 familiar with the open fetal repair which is similar to the postnatal repair. On the other hand,
209 fetoscopy introduces new challenges such as lack of depth perception, constrained tissue
210 handling and suturing which can be simulated using our model. Study of the learning curve
211 of clinical spina bifida repair has shown that experience reduces operation time even in
212 experience endoscopic surgeons, and that training for fetoscopic repair takes longer. Pre-
213 operative practice/rehearsal has been shown to reduce operation time ^{19,37}, port placement,
214 team building, and standardization of the technique. Our model is an addition to the
215 available tools, that concentrates on the neurosurgical steps, which are more complex when
216 the repair is done by fetoscopy.

217 To ensure the acquisition of correct surgical technique and get appropriate advice, it seems
218 logical that any training is proctored by a surgeon familiar with this clinical procedure.

219 *Research implications*

220 Three experienced laparoscopic surgeons participated in our simulation and demonstrated
221 reasonable competency in transferring their endoscopic skills. Further studies can explore
222 skill improvement and the acquisition and retention of skills for novice endoscopic surgeons.

223 The model's logistical and ethical advantages make it possible to investigate complex
224 research questions without relying heavily on animal experiments. This training model has
225 the potential to aid in the development of new surgical instruments and facilitate
226 comparisons of techniques, including robotic surgery. Our immediate goal is to compare the
227 performance of robotic systems to straight stick laparoscopy, especially for neurosurgeons
228 without laparoscopy training. Previous studies have shown that non-endoscopic surgeons
229 learn robotic surgery faster than straight stick laparoscopy³⁸. We also aim to utilize the
230 model for training robotic repair to mitigate the lack of haptic feedback. Additionally, we
231 plan to evaluate stereo versus monocular fetoscopy and explore the use of single-port
232 surgical robotics^{39, 40}. While a robotic approach may already reduce stresses on the uterine
233 walls due to the remote center of motion, the use of a single (as opposed to multiple ports)
234 robot may reduce that even further⁴¹. Data generated from experiments can contribute to
235 extensive datasets for deep learning algorithms, including tool segmentation⁴², skill analysis
236⁴³, and anomaly detection⁴⁴. The model's clean, fast, and portable setup enables training and
237 demonstrations at conferences, facilitating knowledge dissemination and advancing surgical
238 research.

239 *Strengths and limitations*

240 The synthetic model is ideal for desktop dry-lab training due to its easy setup and quick
241 preparation. It can be securely mounted on any surface using a clamp, and the adjustable
242 surgical beds allow for versatile orientations. The model is cost-effective and ethically sound.
243 Its portable design facilitates use in multi-centric trainings and knowledge sharing. The
244 model further facilitates joint training of surgeons and their team leading to effective
245 teamwork, coordination, and communication. Additionally, the model has the potential for
246 water filling, enabling ultrasound scanning and guided port insertion. Manufacturing the

247 model is straightforward with a 3D printer, allowing customization based on patient-specific
248 needs.

249 However, it's important to note that the synthetic silicone material cannot perfectly
250 replicate the fragility and fidelity of fetal structures. The model also lacks specific procedural
251 steps like ultrasound assessment to assist in entry point determination and fetal positioning,
252 appropriate cannula insertions, fetal membranes fixation, compromised vision due to in-
253 utero humidity, an additional abdominal cavity, and suturing of fetal membranes at the end
254 of the procedure. Also the model was evaluated by three expert surgeons. However, to
255 establish it's generalizability, it is imperative to conduct further testing with surgeons of
256 varying levels of experience. Lastly, the manufacturing process may be time-consuming (50
257 min per model), but efficiency can be enhanced by producing models in batches.

258 **CONCLUSIONS**

259 We have created a synthetic high-fidelity and low-cost model that is capable of mimicking
260 the neurosurgical steps fetoscopic spina bifida repair. We report on its use by three
261 experienced laparoscopic surgeons using either straight stick or robot-assisted (Da Vinci Xi)
262 instruments. We propose its further use for measuring the learning curve of novices and the
263 retention of operative skills.

264

265 **Author's Contributions**

266 **Mirza A. Ahmad:** Conceptualization, Methodology, Formal analysis, Data curation, Model
267 creation, Writing – Original draft. **Luc Joyeux:** Conceptualization, Methodology, Writing –
268 Original draft. **Kanokwaroon Watananirun:** Fetoscopy assistance. **Felix De Bie:** OSATS scoring. **Ann-**
269 **Sophie Page:** Expert surgeon, Writing – Review & editing. **Paolo De Coppi:** Expert surgeon, Writing

270 – Review & editing. **Tom Vercauteren:** Supervision, Writing – Review & editing. **Emmanuel**

271 **Vander Poorten:** Supervision, Writing – Review & editing. **Jan Deprest:** Conceptualization,

272 Methodology, Supervision, Writing – Review & editing.

273 **Acknowledgements**

274 J Deprest is funded by the Great Ormond Street Charity fund.

275 **REFERENCES**

- 276 1. Joyeux L, Danzer E, Flake AW, Deprest J. Fetal surgery for spina bifida aperta. *Arch Dis Child*
277 *Fetal Neonatal Ed.* 2018;103(6):F589-F595. doi:10.1136/ARCHDISCHILD-2018-315143
- 278 2. Brock JW, Thomas JC, Baskin LS, et al. Effect of Prenatal Repair of Myelomeningocele on
279 Urological Outcomes at School Age. *J Urol.* 2019;202(4):812-818.
280 doi:10.1097/JU.0000000000000334
- 281 3. Houtrow AJ, Thom EA, Fletcher JM, et al. Prenatal Repair of Myelomeningocele and School-
282 age Functional Outcomes. *Pediatrics.* 2020;145(2). doi:10.1542/PEDS.2019-1544
- 283 4. Farmer DL, Thom EA, Brock JW, et al. The Management of Myelomeningocele Study: full
284 cohort 30-month pediatric outcomes. *Am J Obstet Gynecol.* 2018;218(2):256.e1-256.e13.
285 doi:10.1016/J.AJOG.2017.12.001
- 286 5. Houtrow AJ, MacPherson C, Jackson-Coty J, et al. Prenatal Repair and Physical Functioning
287 Among Children With Myelomeningocele: A Secondary Analysis of a Randomized Clinical Trial.
288 *JAMA Pediatr.* 2021;175(4). doi:10.1001/JAMAPEDIATRICS.2020.5674
- 289 6. Adzick NS, Thom EA, Spong CY, et al. A Randomized Trial of Prenatal versus Postnatal Repair of
290 Myelomeningocele. *New England Journal of Medicine.* 2011;364(11):993-1004.
291 doi:10.1056/NEJMoa1014379
- 292 7. Joyeux L, Engels AC, Russo FM, et al. Fetoscopic versus Open Repair for Spina Bifida Aperta: A
293 Systematic Review of Outcomes. *Fetal Diagn Ther.* 2016;39(3):161-171.
294 doi:10.1159/000443498
- 295 8. Botelho RD, Imada V, Rodrigues Da Costa KJ, et al. Fetal Myelomeningocele Repair through a
296 Mini-Hysterotomy. *Fetal Diagn Ther.* 2017;42(1):28-34. doi:10.1159/000449382
- 297 9. Peralta CFA, Botelho RD, Romano ER, et al. Fetal open spinal dysraphism repair through a
298 mini-hysterotomy: Influence of gestational age at surgery on the perinatal outcomes and
299 postnatal shunt rates. *Prenat Diagn.* 2020;40(6):689-697. doi:10.1002/PD.5675
- 300 10. Sanz Cortes M, Chmait RH, Lapa DA, et al. Experience of 300 cases of prenatal fetoscopic open
301 spina bifida repair: report of the International Fetoscopic Neural Tube Defect Repair
302 Consortium. *Am J Obstet Gynecol.* 2021;225(6):678.e1-678.e11.
303 doi:10.1016/J.AJOG.2021.05.044
- 304 11. Chmait RH, Monson MA, Pham HQ, et al. Percutaneous/mini-laparotomy fetoscopic repair of
305 open spina bifida: a novel surgical technique. *Am J Obstet Gynecol.* 2022;227(3):375-383.
306 doi:10.1016/J.AJOG.2022.05.032
- 307 12. Belfort MA, Whitehead WE, Shamshirsaz AA, et al. Fetoscopic open neural tube defect repair:
308 Development and refinement of a two-port, carbon dioxide insufflation technique. *Obstetrics*
309 *and Gynecology.* 2017;129(4):734-743. doi:10.1097/AOG.0000000000001941
- 310 13. Lapa DA. Endoscopic fetal surgery for neural tube defects. *Best Pract Res Clin Obstet*
311 *Gynaecol.* 2019;58:133-141. doi:10.1016/J.BPOBGYN.2019.05.001
- 312 14. Joyeux L, De Bie F, Danzer E, et al. Learning curves of open and endoscopic fetal spina bifida
313 closure: systematic review and meta-analysis. *Ultrasound in Obstetrics & Gynecology.*
314 2020;55(6):730-739. doi:10.1002/UOG.20389

- 315 15. Anastakis DJ, Regehr G, Reznick RK, et al. Assessment of technical skills transfer from the
316 bench training model to the human model. *The American Journal of Surgery*. 1999;177(2):167-
317 170. doi:10.1016/S0002-9610(98)00327-4
- 318 16. Joyeux L, Javaux A, Eastwood MP, et al. Validation of a high-fidelity training model for
319 fetoscopic spina bifida surgery. *Sci Rep*. 2021;11(1):6109.
- 320 17. Joyeux L, De Bie F, Danzer E, Van Mieghem T, Flake AW, Deprest J. Safety and efficacy of fetal
321 surgery techniques to close a spina bifida defect in the fetal lamb model: A systematic review.
322 *Prenat Diagn*. 2018;38(4):231-242.
- 323 18. Michejda M. Intrauterine treatment of spina bifida: primate model. *Zeitschrift für*
324 *Kinderchirurgie*. 1984;39(04):259-261.
- 325 19. Miller JL, Ahn ES, Garcia JR, Miller GT, Satin AJ, Baschat AA. Ultrasound-based three-
326 dimensional printed medical model for multispecialty team surgical rehearsal prior to
327 fetoscopic myelomeningocele repair. *Ultrasound in Obstetrics & Gynecology*. 2018;51(6):836-
328 837. doi:10.1002/UOG.18891
- 329 20. Belfort MA, Whitehead WE, Bednov A, Shamshirsaz AA. Low-fidelity simulator for the
330 standardized training of fetoscopic meningomyelocele repair. *Obstetrics and Gynecology*.
331 2018;131(1):125-129. doi:10.1097/AOG.0000000000002406
- 332 21. Spoor JKH, van Gastel L, Tahib F, et al. Development of a simulator for training of fetoscopic
333 myelomeningocele surgery. *Prenat Diagn*. Published online March 1, 2023.
334 doi:10.1002/PD.6308
- 335 22. Adzick NS, Thom EA, Spong CY, et al. A Randomized Trial of Prenatal versus Postnatal Repair of
336 Myelomeningocele. *New England Journal of Medicine*. 2011;364(11):993-1004.
337 doi:10.1056/NEJMoa1014379
- 338 23. Farmer DL, Thom EA, Brock JW, et al. The Management of Myelomeningocele Study: full
339 cohort 30-month pediatric outcomes. *Am J Obstet Gynecol*. 2018;218(2):256.e1-256.e13.
340 doi:10.1016/J.AJOG.2017.12.001
- 341 24. Joyeux L, De Bie F, Danzer E, et al. Learning curves of open and endoscopic fetal spina bifida
342 closure: systematic review and meta-analysis. *Ultrasound in Obstetrics & Gynecology*.
343 2020;55(6):730-739. doi:10.1002/UOG.20389
- 344 25. Belfort MA, Whitehead WE, Shamshirsaz AA, et al. Fetoscopic open neural tube defect repair:
345 Development and refinement of a two-port, carbon dioxide insufflation technique. *Obstetrics*
346 *and Gynecology*. 2017;129(4):734-743. doi:10.1097/AOG.0000000000001941
- 347 26. Joyeux L, van der Merwe J, Aertsen M, et al. Neuroprotection is improved by watertightness
348 of fetal spina bifida repair in the sheep model. *Ultrasound Obstet Gynecol*. 2023;61(1):81-92.
349 doi:10.1002/UOG.24907
- 350 27. Avery RA, Shah SS, Licht DJ, et al. Reference Range for Cerebrospinal Fluid Opening Pressure in
351 Children. *New England Journal of Medicine*. 2010;363(9):891-893.
352 doi:10.1056/NEJMC1004957/SUPPL_FILE/NEJMC1004957_DISCLOSURES.PDF
- 353 28. Martin JA, Regehr G, Reznick R, et al. Objective structured assessment of technical skill
354 (OSATS) for surgical residents. *British Journal of Surgery*. 1997;84(2):273-278.
355 doi:10.1046/J.1365-2168.1997.02502.X

- 356 29. Salomon LJ, Bernard JP, Ville Y. Estimation of fetal weight: reference range at 20–36 weeks'
357 gestation and comparison with actual birth-weight reference range. *Ultrasound in Obstetrics*
358 *and Gynecology*. 2007;29(5):550-555. doi:10.1002/UOG.4019
- 359 30. Grantcharov TP, Kristiansen VB, Bendix J, Bardram L, Rosenberg J, Funch-Jensen P.
360 Randomized clinical trial of virtual reality simulation for laparoscopic skills training. *British*
361 *Journal of Surgery*. 2004;91(2):146-150. doi:10.1002/BJS.4407
- 362 31. Grober ED, Hamstra SJ, Wanzel KR, et al. The Educational Impact of Bench Model Fidelity on
363 the Acquisition of Technical Skill: The Use of Clinically Relevant Outcome Measures. *Ann Surg*.
364 2004;240(2):374. doi:10.1097/01.SLA.0000133346.07434.30
- 365 32. Chandrasekera SK, Donohue JF, Orley D, et al. Basic Laparoscopic Surgical Training:
366 Examination of a Low-Cost Alternative. *Eur Urol*. 2006;50(6):1285-1291.
367 doi:10.1016/J.EURURO.2006.05.052
- 368 33. Brydges R, Carnahan H, Rose D, Rose L, Dubrowski A. Coordinating progressive levels of
369 simulation fidelity to maximize educational benefit. *Acad Med*. 2010;85(5):806-812.
370 doi:10.1097/ACM.0B013E3181D7AABD
- 371 34. Tun JK, Alinier G, Tang J, Kneebone RL. Redefining Simulation Fidelity for Healthcare
372 Education. *Simul Gaming*. 2015;46(2):159-174.
373 doi:10.1177/1046878115576103/ASSET/IMAGES/LARGE/10.1177_1046878115576103-
374 FIG2.JPEG
- 375 35. Belfort MA, Whitehead WE, Bednov A, Shamshirsaz AA. Low-Fidelity Simulator for the
376 Standardized Training of Fetoscopic Meningomyelocele Repair. *Obstetrics and gynecology*.
377 2018;131(1):125-129. doi:10.1097/AOG.0000000000002406
- 378 36. Demi B, Ortmaier T, Seibold U. The touch and feel in minimally invasive surgery. *HAVE 2005:*
379 *IEEE International Workshop on Haptic Audio Visual Environments and their Applications*.
380 2005;2005(October):33-38. doi:10.1109/HAVE.2005.1545648
- 381 37. Nakayama K, Oshiro Y, Miyamoto R, Kohno K, Fukunaga K, Ohkohchi N. The Effect of Three-
382 Dimensional Preoperative Simulation on Liver Surgery. *World J Surg*. 2017;41(7):1840-1847.
383 doi:10.1007/S00268-017-3933-7/FIGURES/4
- 384 38. Leijte E, de Blaauw I, Van Workum F, Rosman C, Botden S. Robot assisted versus laparoscopic
385 suturing learning curve in a simulated setting. *Surg Endosc*. 2020;34(8):3679-3689.
386 doi:10.1007/S00464-019-07263-2
- 387 39. Sinha R, Sundaram M, Raje S, Rao G, Sinha M, Sinha R. 3D laparoscopy: Technique and initial
388 experience in 451 cases. *Gynecol Surg*. 2013;10(2):123-128. doi:10.1007/S10397-013-0782-
389 8/FIGURES/5
- 390 40. Moschovas MC, Bhat S, Rogers T, et al. Applications of the da Vinci single port (SP) robotic
391 platform in urology: a systematic literature review. *Minerva Urology and Nephrology*.
392 2020;73(1):6-16. doi:10.23736/S2724-6051.20.03899-0
- 393 41. Locke RCO, Patel R V. Optimal remote center-of-motion location for robotics-assisted
394 minimally-invasive surgery. *Proc IEEE Int Conf Robot Autom*. Published online 2007:1900-
395 1905. doi:10.1109/ROBOT.2007.363599

- 396 42. Madad Zadeh S, Francois T, Calvet L, et al. SurgAI: deep learning for computerized
397 laparoscopic image understanding in gynaecology. *Surg Endosc.* 2020;34:5377-5383.
- 398 43. Lam K, Chen J, Wang Z, et al. Machine learning for technical skill assessment in surgery: a
399 systematic review. *NPJ Digit Med.* 2022;5(1):24.
- 400 44. Reiter W. Video anomaly detection in post-procedural use of laparoscopic videos. In:
401 *Bildverarbeitung Für Die Medizin 2020: Algorithmen–Systeme–Anwendungen. Proceedings*
402 *Des Workshops Vom 15. Bis 17. März 2020 in Berlin.* Springer; 2020:101-106.
- 403
- 404

405 **TABLES**

406 **Table 1:** Comparison of 10 steps in a clinical spina bifida fetoscopic repair as described by
 407 Belfort *et al.*¹² and a simulated fetoscopic repair in the silicon model.

408

	Surgical steps	Clinical fetoscopic repair	Simulated fetoscopic repair
1	Uterine exposition	Exteriorization, exposition and keeping the uterus moistened	Not simulated. Uterus is mimicked by a silicon ball.
2	Uterine access	Transmyometrial membrane fixation, cannulated uterine access via Seldinger-technique under ultrasound guidance	Incisions are made in the silicon ball, ports are inserted and sutured to the silicon.
3	Creating workspace	CO ₂ pneumamnion	Air-tight seal allows the silicon ball to be pressurized/insufflated by CO ₂ .
4	Exposition of target area	Fetal manipulation by instruments to provide access to the lumbar region	Target area is present in form of a cyst on the removable silicon plate. The cyst is filled with water to mimic presence of CSF.
5	Dissection	Dissection of the placode to completely untether it.	Dissection of the placode to completely untether it. Access skin around placode is removed.
6	Tissue resection and undermining	Circumferential resection of the junction line and undermining of the skin.	Circumferential undermining of the mid-line feature (oval gap in layer-2).
7	Tissue mobilization	Approximation of lumbar skin edges	Pulling of the undermined flaps of layer-2 over the placode and approximating them in the middle.
8	Closure of the first layer	Dissection and suturing of myo-fascial flaps with/without patch	Suturing the layer-2 flaps.
9	Closure of the second layer	Fetal skin closure with running sutures.	Circumferential undermining of the skin (layer-3) and closure with running sutures.
10	Quality assessment of the repair	Quality assessment of the skin suture line by inspection and adjustment.	Inspection of the suture line and closure quality by water tightness test.

409

410 **Table 2:** Cost of the spina bifida training model. The cost for 3D printed parts depends on the
 411 local 3D printing service provider (0.1€/g for this study). All the Computer-Aided Design (CAD)-
 412 files (.stl format) are provided as supplementary material for 3D printing, which saves
 413 engineering costs. As the cost of working hours vary from place to place, only time use is
 414 reported.

Initial one-time cost:		
Part	Source	Cost (€)
Base	<i>base.stl</i> , 3D print PLA (207g)	20.7
Uterine ring	<i>ring.stl</i> , 3D print PLA (126g)	12.6
Silicon hump mold	<i>hump.stl</i> , 3D print PLA (87g)	8.7
Skin mold top	<i>skin_top.stl</i> , 3D print PLA (40g)	4
Skin mold bottom	<i>skin_bottom.stl</i> , 3D print PLA (80g)	8
Fascia mold	<i>fascia.stl</i> , 3D print PLA (65g)	6.5
Layer_1 mold	<i>layer_1.stl</i> , 3D print PLA (60g)	6
Cyst template	<i>template.stl</i> , 3D print PLA (4g)	0.4
Uterine ball mold inner shell	<i>uterine_ball_inner.stl</i> , 3D print PLA, (340g)	34
Uterine ball mold outer shell	<i>uterine_ball_outer.stl</i> , 3D print PLA, (4x115g)	46
Quick release clamp	Hardware store	3
Hose clamp	Hardware store	5
Uterine ball	Ecoflex 00-30 Silicon, 300g	~17.2
Silicon hump	Ecoflex 00-30 Silicon, 120g	~6.9
Silicon pigments	Smooth-on SilPig, 9 sample pack	31
Gauze	Kompres Medi S30 Gauze, 7.5x7.5	1
Total		211
Cost of one removable model of a myelomeningocele lesion:		

Layer_1	Ecoflex 00-30 Silicon, 35g	2
Fascia	Ecoflex 00-30 Silicon, 40g	2.3
Skin	Ecoflex 00-30 Silicon, 40g	2.3
Gel	Ecoflex Gel, ~8g	~0.44
Infuser tube	Braun Perfusor Line, 0.9MMx150CM, PE	2.5 (recyclable)
Time	0.8 hours	N.R.
Total		22
One time engineering and design cost incurred by the authors		400 wage hours + 1000 euros in materials

415

416

417

418

419

420

421

422

423

424

425

426

427

428

429

430

431

432

433

434
435
436
437
438
439
440
441

FIGURES

442 **Figure 1:** Setup for the model for simulated fetoscopic spina bifida repair. (a)
443 Cross-sectional view of the three-layer single-use myelomeningocele (MMC)
444 lesion, (b) the 3D-printed ring clamps the model of the lesion to the 3D-printed
445 base, (c) silicon ball, mimicking the exposed uterus, is placed around the
446 threaded ring and clamped to it by a hose clamp, creating an air-tight simulated
447 uterine environment. The base is fixed to a surgical bed using a quick release
448 clamp. (d) Set up during the exercise with ports for right and left hand
449 instruments and fetoscope inserted, (e) Set up during the robot assisted repair
450 exercise with instrument ports in place.

451
452 **Figure 2:** Comparison of essential steps performed during a clinical (A-E) and a
453 simulated fetoscopic spina bifida repair in the silicon model (F-J).

454
455 **Figure 3:** First row displays the time taken by each surgeon for the surgical
456 steps, as well as the total time. On top of each bar the colored circle indicates
457 whether there is leakage (red) or not (green). The second row displays the CO₂
458 used during the entire exercise. The third row plots the objective structured
459 assessment of technical skill (OSATS) scores as given by an independent
460 surgeon blinded to the operator and the sequence. The dotted line (score: 18)
461 represents the cut off. The last row displays the competitive CUSUM analysis
462 scores. The dotted line represents the competitive control limit ($h_c = 3$), staying
463 below this line indicates surgeon's competency. Red bars are indicative of
464 surgical failure of the trial in the given category.

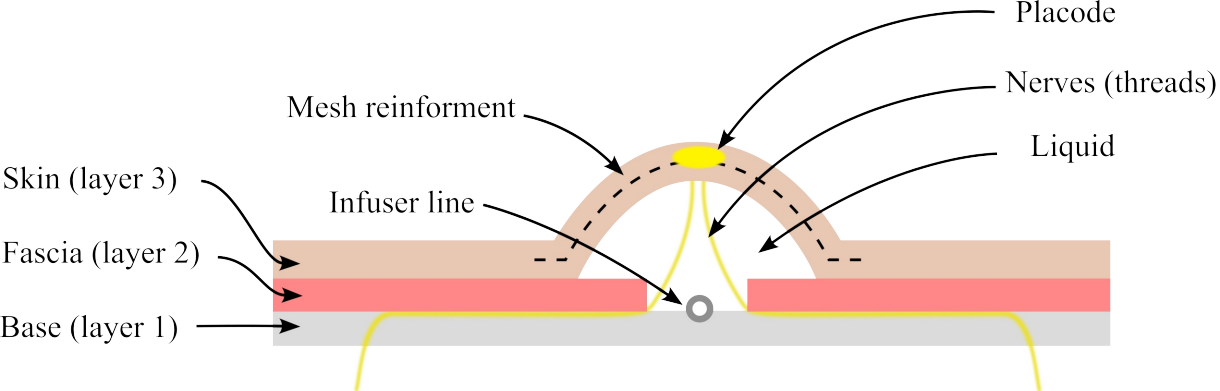
465

466 **Video 1:** The installation setup of the synthetic spina bifida repair model.
467 Fetoscopic view of a 3-port manual repair and a robot assisted repair using a Da
468 Vinci Xi.

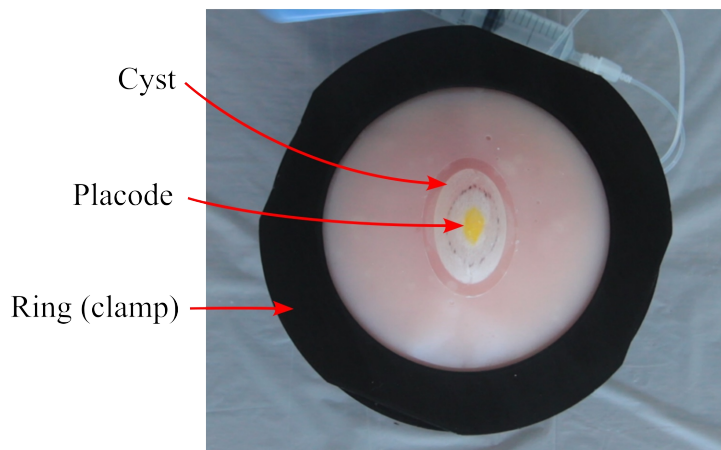
469

470 **Video 2:** Fabrication tutorial of the synthetic spina bifida repair model.

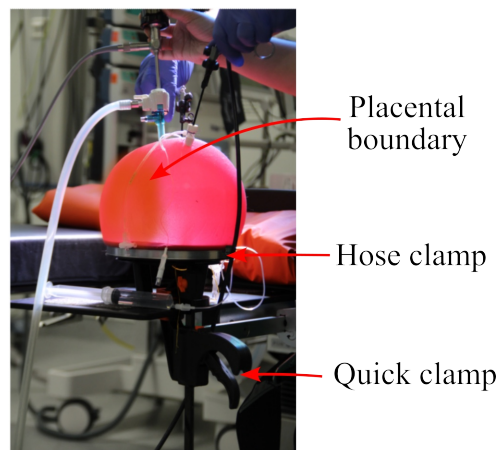
471



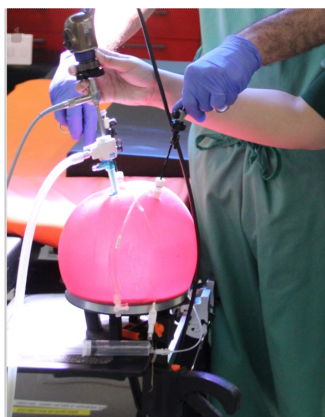
(a)



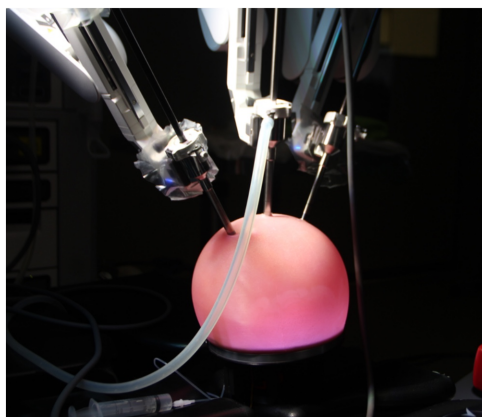
(b)



(c)



(d)



(e)

Clinical surgical target

Simulated surgical target

